Supplementary Figure S1 | a, WB analysis showing the expression level of dLRRK in *Da-Gal4* driven WT, I1915T and 3KD forms of dLRRK transgenics compared to *Da-Gal4/+* non-transgenic control. Tubulin serves as loading control. **b**, **c**, RT-PCR (**b**) and qRT-PCR (**c**) analyses showing equal *gfp* mRNA level in *Da-Gal4>EGFP-let-7-3′UTR* fly heads co-expressing WT, I1915T, 3KD forms of dLRRK, or heterozygous for *ago1* and *dicer1*. *RP-49* mRNA level serves as a control for **b** and **c**.

Supplementary Figure S2 | a, reporter assay using a renilla luciferase construct harbouring six incomplete let-7-binding sites in the 3′UTR. The co-transfected miRNA and hLRRK2 constructs are indicated. The level of *luciferase* mRNA was quantified by RT-PCR. Luciferase activity was normalized with mRNA level (**P*<0.05, *n*=3). **b,** reporter assay using a renilla luciferase construct harbouring six incomplete let-7-binding sites in the 3′UTR. The co-transfected miRNA and Flag-tagged hLRRK2 constructs are indicated. G2019S-3KD and I2020T-3KD contain combined kinase-inactivating mutations to abolish kinase activity in hLRRK2-G2019S and -I2020T. The data represents three independent experiments (**P<0.05*, *n*=3). **c,** statistical analysis of immunostaining of TH+ neurons in *Ddc-Gal4* driven WT, R1069G and I1915T forms of dLRRK compared to *Ddc-Gal4/+* control (**P<0.05*, *n*=8). Flies were aged for 60 days at 25°C. Note that compared to the *TH-Gal4>dLRRK(I1915T)* transgenic animals (Fig. 2c), *Ddc-Gal4>dLRRK(I1915T)* transgenic animals showed statistically significant DN loss only in PPM1/2 clusters, possibly due to the different strength of the two Gal4 drivers.

Supplementary Figure S3 | Control experiment showing **a,** pathogenic dLRRK did not affect the expression of GFP from a control *EGFP* reporter without let-7 binding sites in the 3′UTR. *Da-Gal4>UAS-GFP* flies were crossed to *UAS-dLRRK(I1915T)* or w^- flies.

GFP signals were acquired by live imaging and signal intensities were quantified; **b,** *TH-Gal4>EGFP-let-7-3′UTR* flies were injected with miR-10 and let-7 miRNA, anti-miR-184*fS and anti-let-7fS antagomirs, or buffer alone into the head. EGFP signals were acquired by live imaging 48 hours post-injection. Bar graphs show signal quantifications (*P<0.05). Values represent mean ± s.d. of six independent experiments. Note that anti-let-7fS injection led to increased EGFP-signal intensities in DN clusters, suggesting that anti-let-7fS interfered with endogenous let-7 function. Injected let-7 miRNA further decreased EGFP-signal intensities in the same DN cluster, indicating increased let-7 function in those neurons. Images in each experiment were acquired and processed with Photoshop under the same settings.

Supplementary Figure S4 | Northern blot analysis of mature miRNA levels in LRRK2 transgenic flies and let-7 pre-miRNA overexpression animals. **a,** Total RNA from *Da-Gal4*-driven hLRRK2(WT), hLRRK2(G2019S), dLRRK(WT), dLRRK(I1915T), and dLRRK(3KD) transgenic flies and *Da-Gal4*/+ control flies were extracted and Northern blot performed. Values represent ratios of endogenous let-7 miRNA level normalized with miR-1 miRNA and standardized with *Da-Gal4/+* control. **b,** Northern blot analysis showing mature let-7 miRNA level after ubiquitous overexpression of pre-let-7 miRNA using *Da-Gal4* driver. Values represent ratios of let-7 miRNA level normalized with *rp49* mRNA level and standardized with *Da-Gal4*/+ control.

Supplementary Figure S5 | **a,** Immunofluorescence analysis showing co-localization of Flag-hLRRK2 and endogenous dAgo1 in DNs in the PAL cluster of 3 day-old animals. *TH-Gal4>hLRRK2* Tg and control *w-* fly heads were co-immunostained for dAgo1 and TH or hLRRK2. Merged images are shown at the bottom. Arrows point to cytoplasmic

punctate structures where hLRRK2 and dAgo1 appear to co-localize. **b,** immunofluorescence staining of TH (red) and dAgo1 (green) in the PPM1/2 cluster of *TH-Gal4*-driven hLRRK2(WT) and hLRRK2(G2019S) transgenic flies and *TH-Gal4*/+ control flies. Merged images are shown at the bottom. Animals are raised at 25°C over 65 days. Note the reduced dAgo1 staining in TH+ neurons expressing hLRRK2.

Supplementary Figure S6 | WB analysis showing the co-IP between hLRRK2 and hAgo-2 or dAgo1 in cell extracts not treated with RNaseA, and the level of dAgo1 in young hLRRK2 transgenic flies. **a,** co-IP of WT, I2020T, G2019S and 3KD forms of hLRRK2 with Flag-tagged hAgo2 after co-transfection into HEK293T cells. IP experiments were performed in extracts without RNase A treatment. **b**, Upper panel: Western blot analysis of HEK293T cells transfected with control siRNA, hLRRK2 siRNA, control plasmid, and hLRRK2(WT) encoding plasmid DNA to show the position and endogenous level of hLRRK2 protein. Tubulin serves as loading control. Lower panel: Western blot analysis of HEK293T cells transfected with different concentrations of hLRRK2 siRNA as indicated and incubated for 72 or 48 hours. Non-treated and hLRRK2(WT) transfected cells serve as controls. Two different batches of the same anti-hLRRK2 antibody (NB300-268SS, Novus) were used for Western blot analysis in the two panels. Longer and shorter exposures are shown. Asterisks mark the position of endogenous hLRRK2. **c,** co-IP between hLRRK2 and dAgo1 in fly head extracts not treated with RNaseA. Flag-tagged hLRRK2 was IPed from *Da-Gal4*-driven transgenics and dAgo1 detected by WB analysis.

Supplementary Figure S7 | Western blot analysis of dAgo1 protein level in various genotypes. **a,** WB analysis of endogenous dAgo1 level in fly head extracts prepared from

3-day old *Da-Gal4>hLRRK2(WT)* and *Da-Gal4>hLRRK2(G2019S)* transgenic animals, or 10-days-old wild type and *dLRRK* mutant flies. Tubulin serves as control (*P<0.05, n=3). **b**, endogenous dAgo1 protein level in *w-* and *ago1* heterozygous animals aged for 41 days at 25°C (*P<0.05, n=3).

Supplementary Figure S8 | Climbing activity assays of the various genotypes after genetic manipulation or miRNA injection. **a,** effects of Dicer1 overexpression or Dicer1 RNAi on the climbing activity of *TH-Gal4>hLRRK2(G2019S)* flies (*$P<0.05$, n=23). **b,** effects of loss of one copy of *ago1* on the climbing activity of *TH-Gal4*-driven *hLRRK2(G2019S)* (left) or *dLRRK(I1915T)* (right) transgenic flies (left, *$P<0.05$, n=6; right, *$P<0.0001$, n=9). **c,** *TH-Gal4*-directed Dicer1 RNAi in *dicer1* heterozygous background leads to reduced locomotor activity (*P<0.0001, n=8). **d,** Dicer1 RNAi effects shown in **c** can be partially rescued by the suppression of dLRRK through RNAi. DN number (left, *$P<0.05$, n=6) and locomoter activity (right, *$P<0.05$, n=7) are shown. Flies were raised at 29°C for 33 days. **e**, effect of overexpression of pre-let-7, pre-miR-184* (left), and injection of let-7, miR-184* (right) on DN number in aged *TH-Gal4>dLRRK(I1915T)* flies compared to *TH-Gal4/+* control. Pre-miR-10, buffer and miR-10 were used as controls. **f,** effects of *dp* or *e2f1* heterozygous background on the climbing activity of *let-7* mutant (*$P<0.05$, n=5). **g,** effects of miRNA injection of wild-type (w^-) flies on DN number (left, $P<0.05$, $n=16$) and climbing activity (right, $n=14$). Buffer and miR-10 injection serve as controls.

Supplementary Figure S9 | DN number and climbing activity assays in various genetic backgrounds or after miRNA manipulation. **a**, effects on DN number (left, *$P<0.05$, n=8) and climbing activity (right, *$P<0.05$, n=16) by anti-let-7fS (2.5 μM) injection into

dLRRK(-/-) and wild-type flies. Injection of anti-let-7mutfS serves as control. **b**, statistical analysis comparing the effects of anti-miR-184*fS antagomir injection (100 μM) on DN number in wild-type vs. *e2f1* or *dp* heterozygous animals (*$P<0.05$, n=6). **c**, effects of antagomir injection (right, 100 μM; left 2.5 μM) at the indicated concentrations on the climbing activity in wild-type vs. *e2f1* or *dp* heterozygous animals (*$P<0.05$, n=15). Anti-let7mutfS injection serves as control. **d,** effect of *Da-Gal4*-driven dp-TP^{control} or dp-TP^{let-7} expression on the climbing activity (*P<0.05, n=11), compared to *TH-Gal4/+* control. **e,** effects of *gDPwt* and *gDPmut* transgene expression on the climbing activity (*P<0.001, n=18) in *Df/dpR217H* background. Flies were raised at 29°C for 33 days. **f**, effects of *elav-Gal4*-driven neuronal overexpression of E2F1 on DN number (left, *P<0.0017, n=8) and locomotor activity (right, *P<0.0001, n=20).

Supplementary Figure S10 | Interaction between LRRK2 and 4E-BP and effects of 4E-BP TE expression on DN number and climbing activity. **a,** co-IP of hAgo2 with h4E-BP(WT) or h4E-BP1(TA) in HEK293T cells. Immunoprecipitation of hAgo2 was performed with anti-Flag antibody. The absence of anti-p-Thr37/46 signal in the h4E-BP1(TA) sample demonstrates specificity of the phospho-antibody. **b,** hLRRK2(G2019S) promotes the association between phospho-4E-BP and hAgo2. 293T cells were triple transfected with hAgo2-Flag and h4E-BP1(WT), together with hLRRK2(WT) or hLRRK2(G2019S). The anti-Flag antibody was used to immunoprecipitate hAgo2. Anti-myc antibody and anti-p-Thr37/46 were used to detect total h4E-BP1 and phospho 4E-BP1, respectively, in the immunocomplex. **c,** dLRRK(I1915T) promotes the association of endogenous phospho-4E-BP and hAgo2. 293T cells were transfected with dLRRK(WT) or dLRRK(I1915T) and endogenous hAgo2 was immunoprecipitated using anti-hAgo2. Anti-p-Thr37/46 and anti-4E-BP1 were used to detect phospho-4E-BP1 and total 4E-BP1 level, respectively, in the immunocomplex. **d**, attenuation of let-7 miRNA

function by d4E-BP(TE) in *m4E-BP1 (-/-)* MEF cells as measured with the renilla-let-7(8x) reporter. The effect of d4E-BP(TE) was abolished when let-7 miRNA was blocked by anti-let-7 (*$P<0.05$, n=4). Luciferase activity levels were normalized with let-7 transfection only or anti-let-7 transfection only controls. Note that MEF cells contain a sufficient level of endogenous let-7 such that let-7 miRNA transfection did not further inhibit reporter suppression when compared to miR-124 control. Consistently, suppression of endogenous let-7 with anti-let-7 led to increased reporter activity when compared to anti-miR-184* control. **e,** WB analysis showing the effects of 4E-BP(WT) and 4E-BP(TE) on the expression of the *EGFP-let-7-3'UTR* or *EGFP* reporter. GFP levels normalized with 4E-BP levels are shown (*P<0.05, n=3). **f,** analysis of DN number (left) and climbing activity (right) in *Da-Gal4*-driven 4E-BP(WT) and 4E-BP(TE) transgenics, compared to *Da-Gal4*/+ control (DN number, *$P<0.05$, n=8; climbing activity, *$P<0.05$, n=21). **g,** DN number (left) and climbing activity (right) of *TH-Gal4*-driven 4E-BP(TE) transgenics compared to *TH-Gal4*/+ control (DN number, *$P<0.01$, n=8; climbing activity, *$P<0.0001$, n=25). **h**, endogenous dAgo1 protein level in head extracts of *Da-Gal4*-driven d4E-BP(TA), d4E-BP(WT), and d4E-BP(TE) transgenics aged for 65 days at 25°C. Actin serves as loading control. **i,** quantification of DN number in *w*- and *ago2* homozygous mutant flies aged for 59 days at 25°C. **j,** WB analysis showing the expression of the *EGFP-let-7-3'UTR* reporter in flies expressing hLRRK2(G2019S) or d4E-BP(TA) alone, or in combination. Tubulin serves as control.

Supplementary Figure S11 | Puromycin treatment showing association of *e2f1* and *dp* mRNA with active polysomes. **a,** WB analysis of sucrose gradient fractions showing co-sedimentation of dLRRK(WT) and dLRRK(I1915T) in polysomal fractions. Fly head extracts are generated from *Da-Gal4* driven transgenenics. dPABP and Tubulin serve as polysomal and non-polysomal controls, respectively. **b,** RT-PCR analysis showing

polysomal association by *e2f1* and *dp* mRNA. Fly head extracts with or without puromycin treatment were fractionated on sucrose gradients and high-density fractions #9 to #14 are pooled, and RNAs extracted. Quantitative RT-PCR analysis was performed to measure the level of *dp* and *e2f1* mRNA in the fractions. RP-49 mRNA level in the total extract serves as loading control.

Supplementary Figure S12 | Effects of various forms of dLRRK on DP protein expression in animals raised at 25°C. **a**, Western blot analysis of endogenous DP protein levels in head extracts of *Da-Gal4*-driven dLRRK(WT), dLRRK(3KD), and dLRRK(I1915T) transgenic animals compared to *Da-Gal4/+* control (*P<0.05, n=3). Actin serves as loading control. Animals were aged for 61 days at 25°C. **b**, endogenous DP levels in head extracts of dLRRK(WT)/+, dLRRK(3KD)/+, dLRRK(I1915T)/+, hLRRK2(WT)/+, and hLRRK2(G2019S)/+, compared to *w-* control. Animals were aged for 61 days at 25°C. Actin serves as loading control. **c,** bar graph showing qRT-PCR analysis of *dp* and *e2f1* mRNA level normalized by *rp49* mRNA level in the indicated genotypes. Flies were raised for 35 day at 29°C. The mRNAs were extracted from fly heads. **d**, qRT-PCR analysis of *dp* and *e2f1* mRNA level in *dLRRK* mutant and wild-type animals.

Supplementary Figure S13 | Effects of removing one copy of *e2f1*, *dp*, or *lkb1* on the hypersensitivity of *Da-Gal4>dLRRK(I1915T)* flies toward paraquat treatments compared to *Da-Gal4/+* control (*P<0.05, n=10).

Supplementary Figure S14 | Control experiment showing the expression of endogenous let-7 miRNA in DNs. Shown are immunohistochemistry for TH and GFP in DNs of adult fly brain from *let-7-C*^{GKI}*/UAS-GFP* and *let-7-C*^{GKI}/+ control animals. Note that let-7 is expressed in TH+ DNs and their surrounding cells.

Supplementary Figure S15 | Control experiments showing relative specificity of antagomir injection, *let-7* mutation, and E2F1 overexpression on DN loss. **a,** statistical analysis showing the lack of effects of antagomir injection on FMRFamide neuron number (n=6). **b,** images showing the differential effects of blocking miRNA function by antagomir injection on the maintenance of DN and FMRFamide neurons. Buffer or anti-let7mutfS injections serve as controls. While DN number was reduced in anti-let-7fs and anti-miR-184*fs injected animals, FMRFamide neurons were not affected. **c,** statistical analysis showing lack of effect by loss of let-7 (Δlet-7) on FMRFamide neuron number. **d,** images showing differential effects of loss of let-7 (Δlet-7) on the maintenance of DN (red) or FMRFamide (green) neurons in the PPM1/2 cluster. **e**, statistical analysis showing lack of effect by *elav-Gal4* driven E2F1 overexpression on the number of FMRFamide neurons.

Supplementary Figure S16 | **a, b,** Alignments showing mutated seed sequences for miR-184* in the *e2f* 3'UTR (**a**) and for let-7 in the *dp* 3'UTR (**b**). **c,** DNA sequences showing potential let-7-binding sites within *dp* 5'UTR and *dp* CDS and the introduced mutations in the seed sequences. **d,** DNA sequences showing binding sites for control and let-7 protector RNAs within *Drosophila dp* 3'UTR starting at the indicated positions: nucleotide 165 (nt165) for the TP^{control} and nucleotide 754 (nt754) for TP^{let-7}. The let-7 protector RNA binding site includes the let-7 seed sequence as shown in red.

Supplementary Figure S17 | Lack of genetic interaction between dLRRK and bantam or miR-14 miRNAs in the fly eye. **a,** effect of *GMR-Gal4*-driven dLRRK(WT) and dLRRK(I1915T) expression in the spinocerebellar ataxia type 3 (Hsap\MJD.tr-Q78)-bantam (banD) background. *GMR-Gal4>Hsap\MJD.tr-Q78* serves as control. **b**, effect of *GMR-Gal4*-driven dLRRK(WT) and dLRRK(I1915T) expression in the *GMR-reaper(rpr); GMR-miR-14* background. *GMR-reaper/+* serves as control. Bantam and miR-14 miRNAs exert protective effects against the toxicity of MJD.tr-Q78 and Reaper, respectively. WT or pathogenic dLRRK did not modify the protective effects of these miRNAs.

Supplementary Figure S18 | Reporter assay and RT-PCR analysis demonstrating the *in vivo* effects of $TP^{let\text{-}7}$. **a**, functionality assay of dp-$TP^{let\text{-}7}$ *in vivo* using *EGFP-dDP-3'UTR* reporter. Embryos collected from *Da-Gal4/+, Da-Gal4>dp-*$TP^{control}$ and *Da-Gal4>dp-*$TP^{let\text{-}7}$ were injection with equal amounts of *pUAST-EGFP-dDP-3'UTR* plasmid. 24 hours post injection, EGFP signals were detected by live imaging and embryos were subsequently pooled for Western blot analysis (*$P<0.001$, n=8). **b**, qRT-PCR analysis of *dp* mRNA level in fly head extracts prepared from *Da-Gal4/+*, *Da-Gal4>dp-*$TP^{control}$ and *Da-Gal4>dp-*$TP^{let\text{-}7}$ animals. *Rp49* mRNA serves as internal control.

Supplementary Figure S19 | Representative images of TH immunostaining of DNs in the PPM1/2 cluster. **a**, TH immunostaining of the indicated genotypes in the dLRRK RNAi/dicer 1 RNAi genetic interaction cross. Animals were raised at 29°C for 33 days. **b**, TH immunostaining of aged *TH-Gal4/+*, *TH-Gal4>dp-*$TP^{control}$, and *TH-Gal4>dp-*

TP$^{let\text{-}7}$ animals. **c**, TH immunostaining of aged *gDPwt*; *dp Df/dp* and *gDPmut*; *dp Df/dp* animals raised at 29°C for 33 days.

Supplementary Table 1 | A list of selected known genes identified by the translational profiling analysis. The folds of polysomal mRNA level changes between *Da-Gal4>dLRRK(I1915T)* and *Da-Gal4*/+ or between *Da-Gal4>dLRRK(I1915T)* and *Da-Gal4*>dLRRK(WT) were shown.

Supplementary Figure 1

a

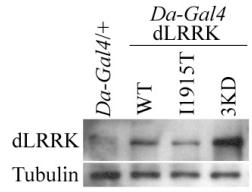

b

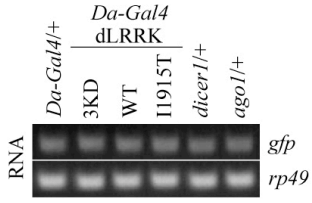

c

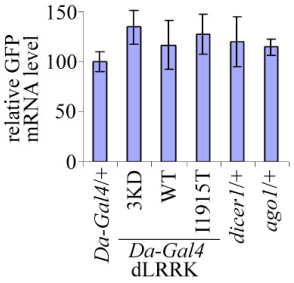

Supplementary Figure 2

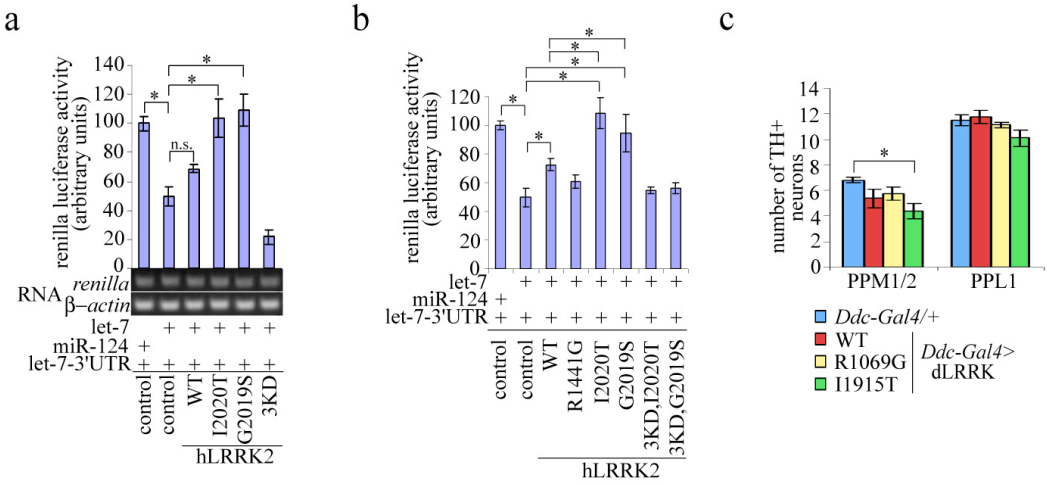

Supplementary Figure 3

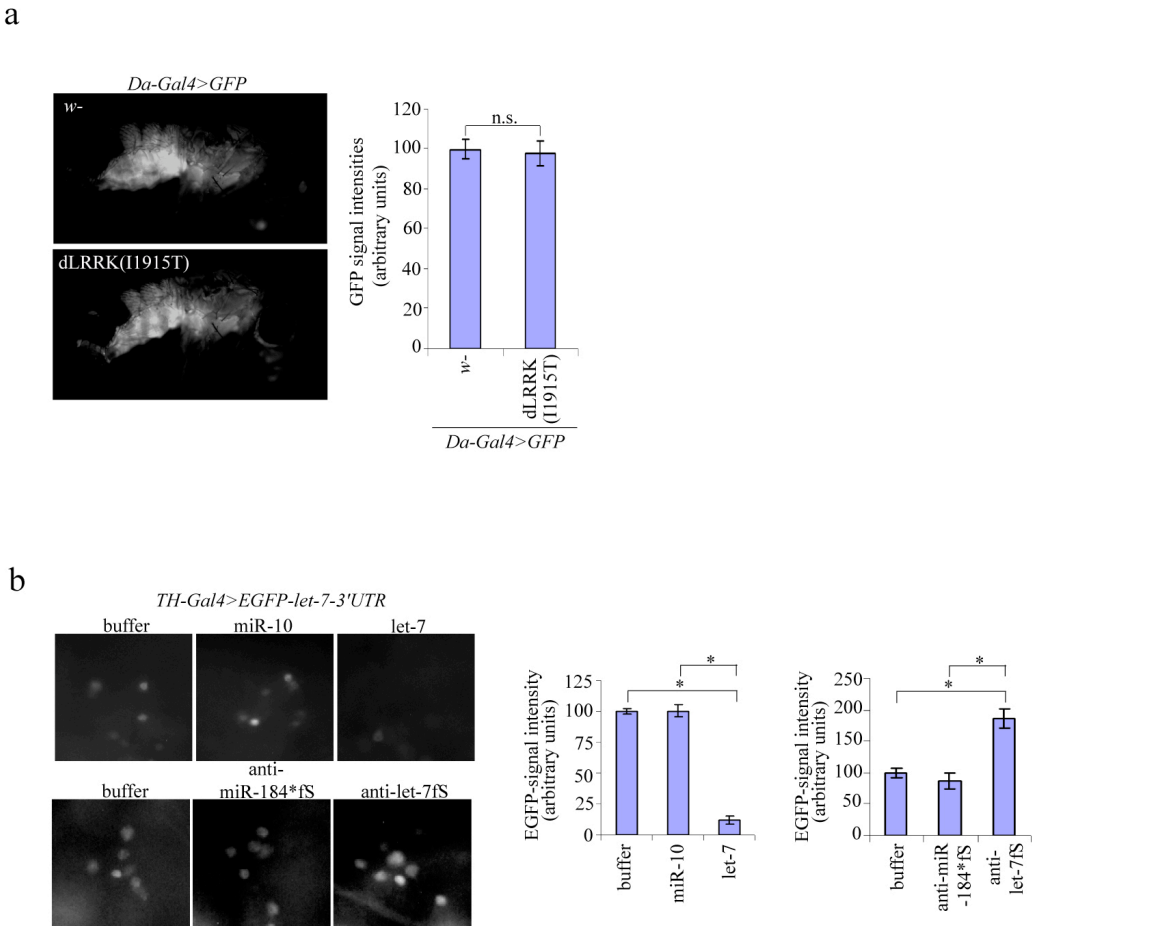

Supplementary Figure 4

a

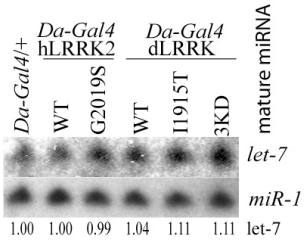

b

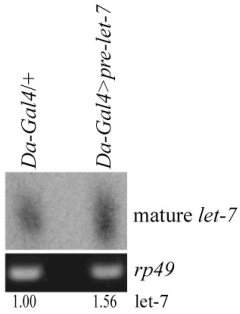

Supplementary Figure 5

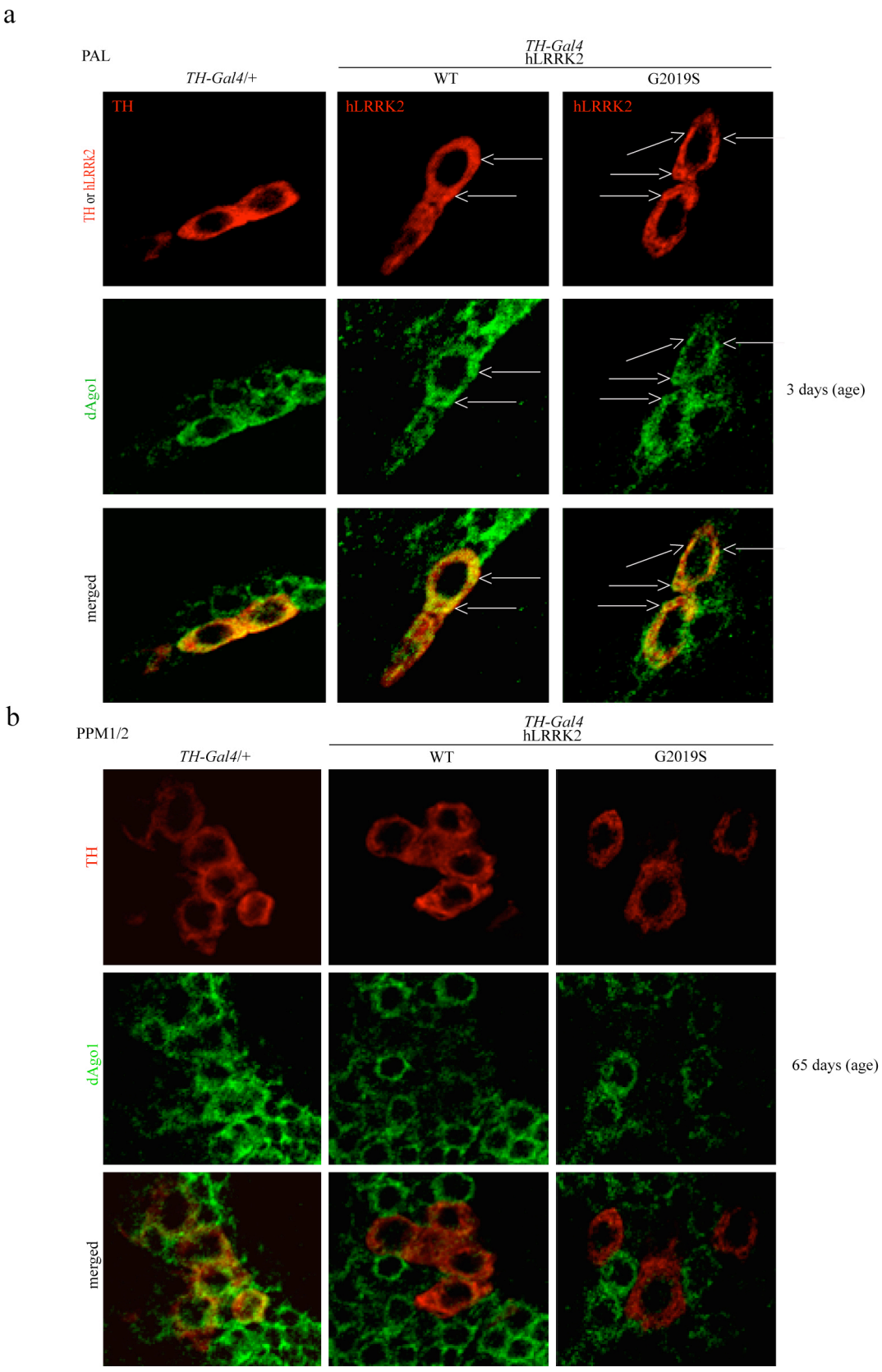

Supplementary Figure 6

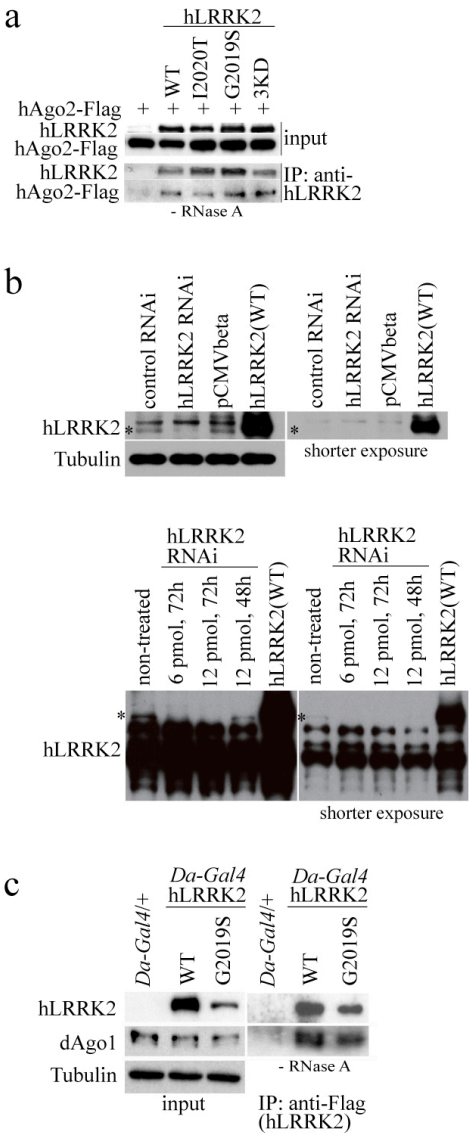

Supplementary Figure 7

a

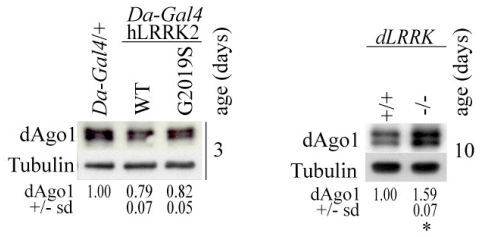

b

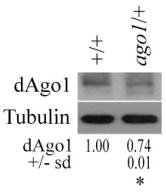

Supplementary Figure 8

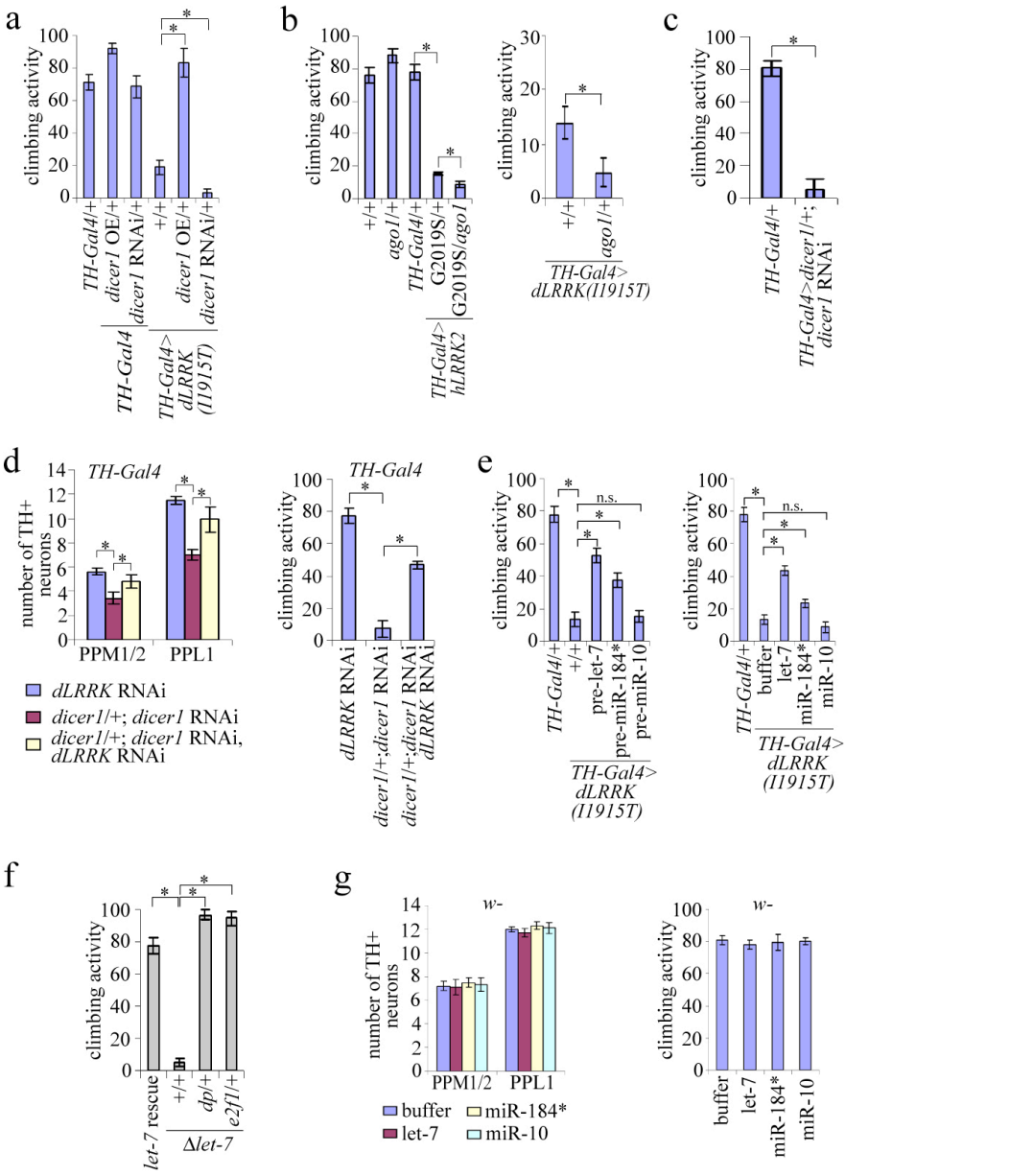

Supplementary Figure 9

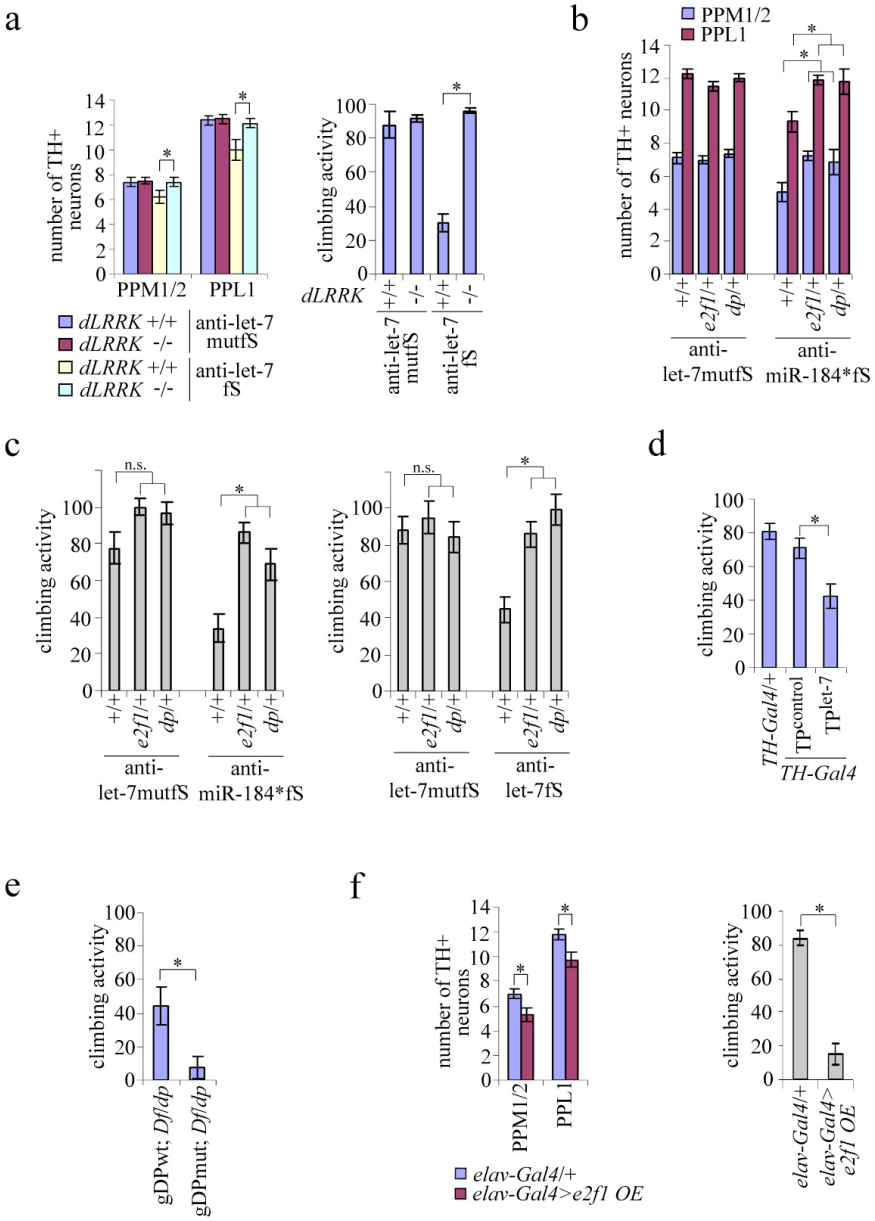

Supplementary Figure 10

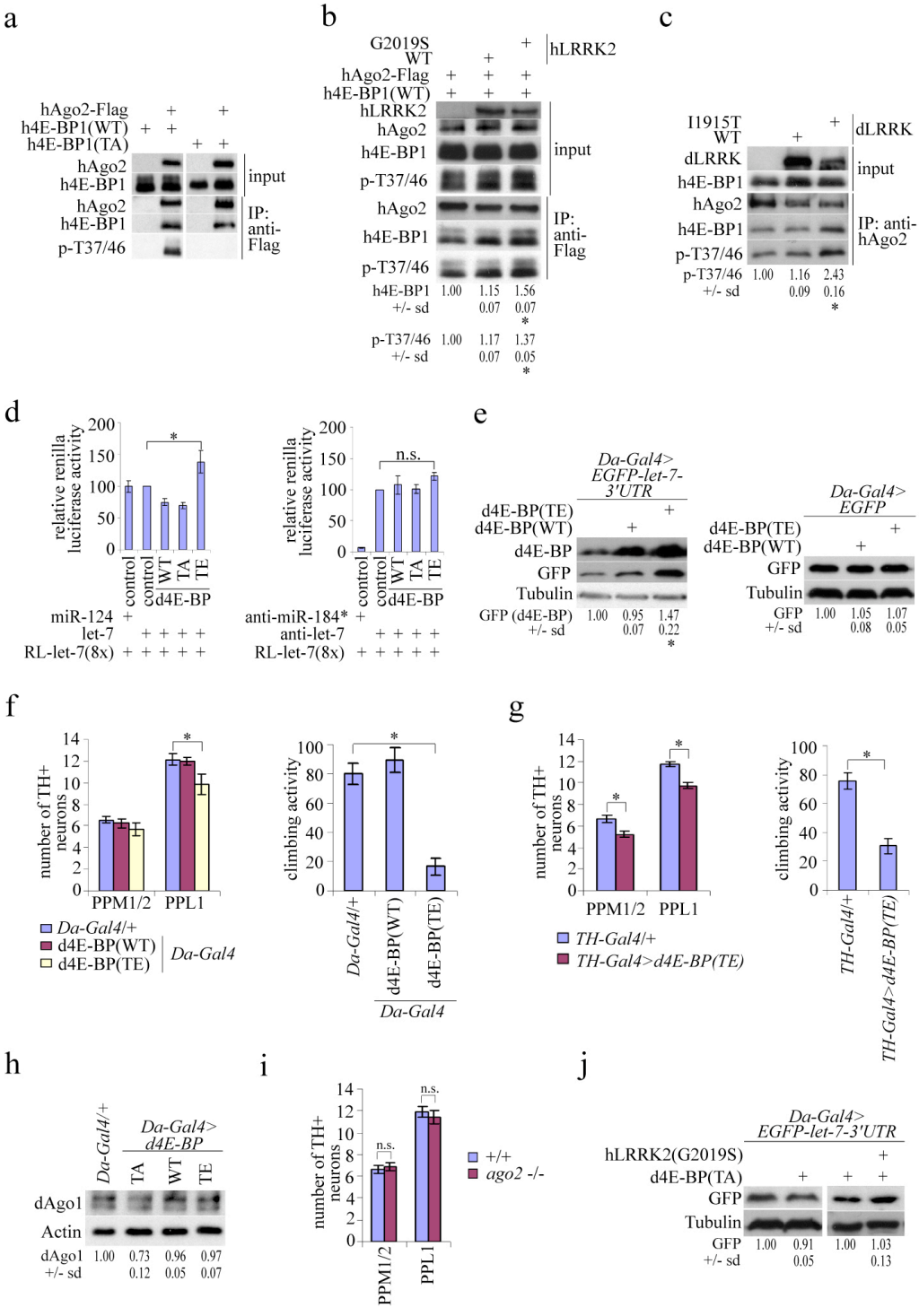

Supplementary Figure 11

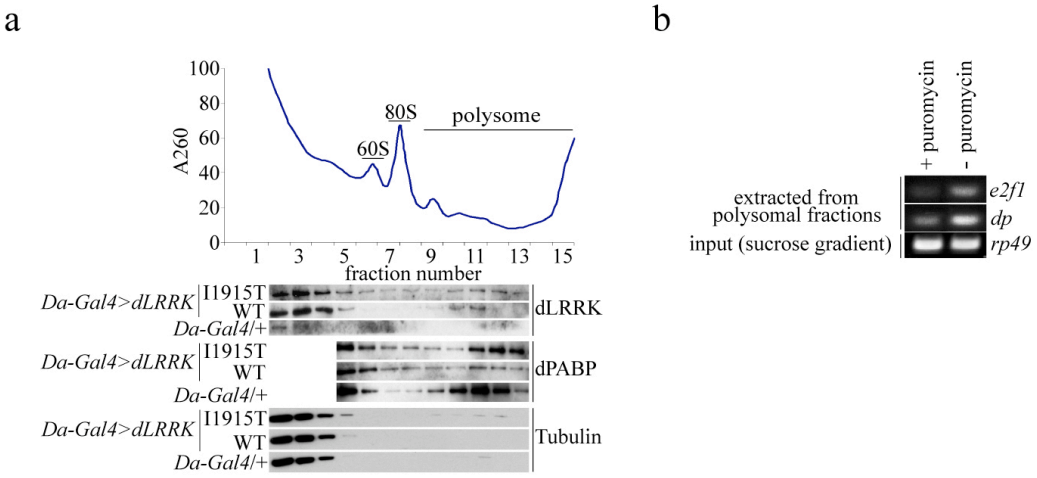

Supplementary Figure 12

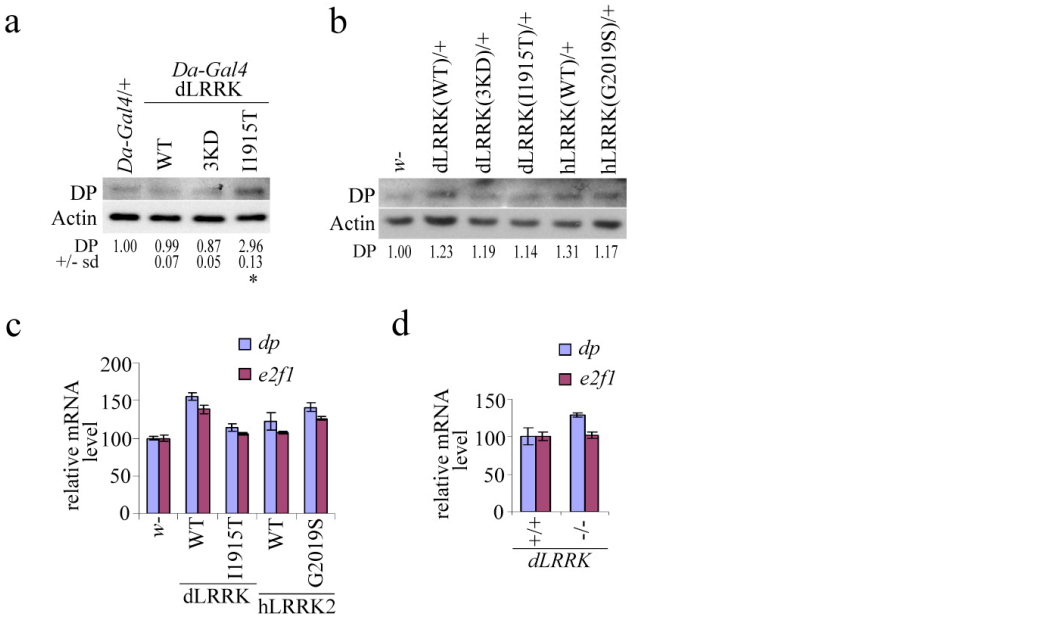

Supplementary Figure 13

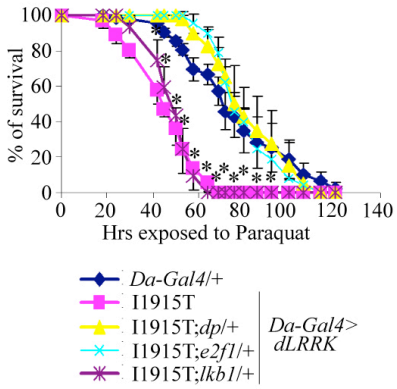

Supplementary Figure 14

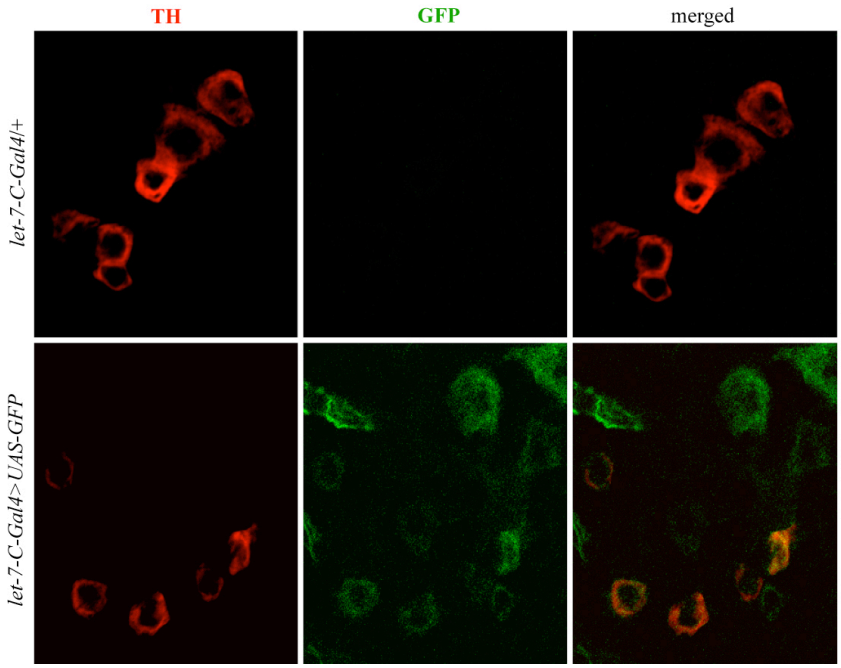

Supplementary Figure 15

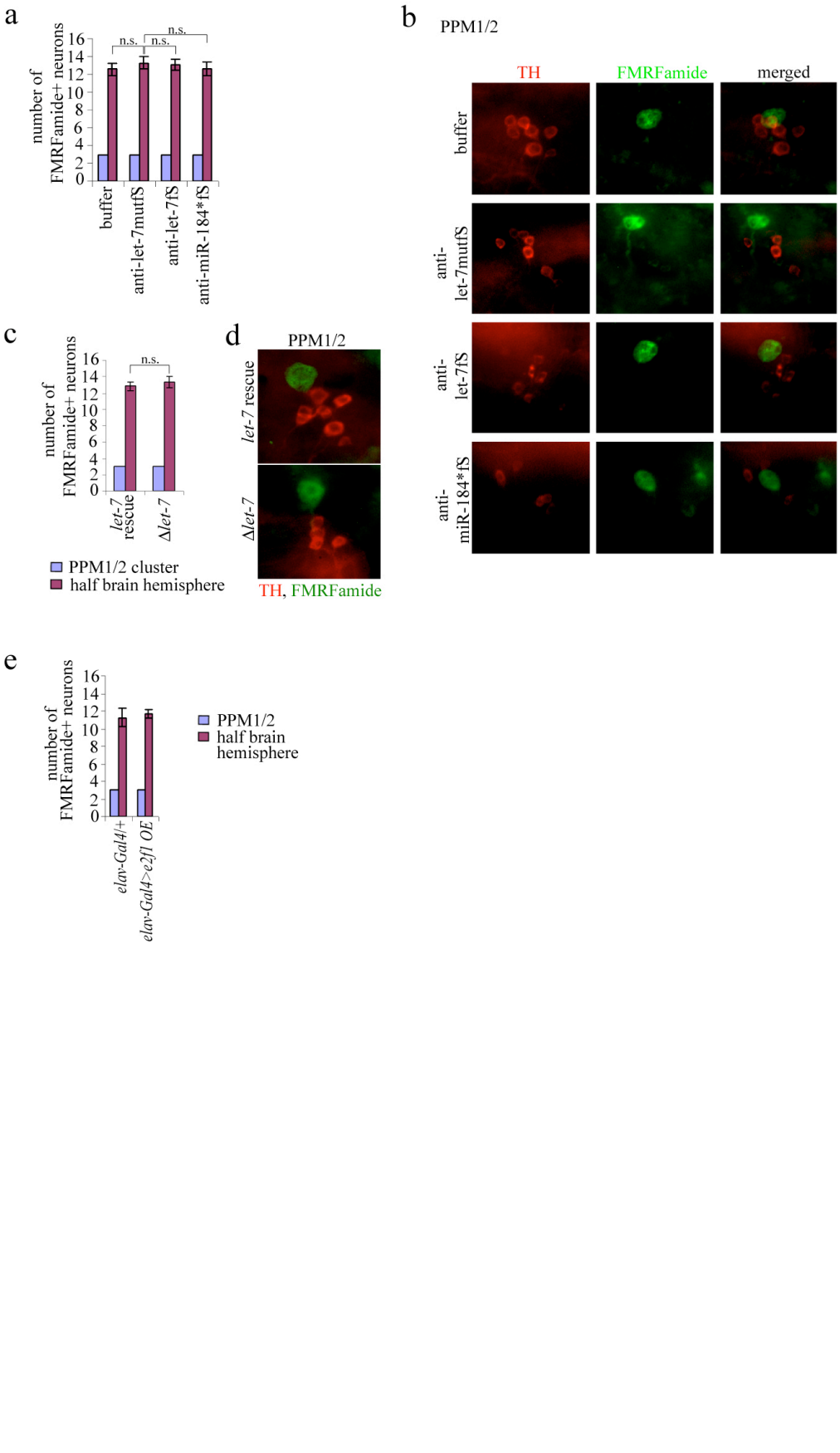

Supplementary Figure 16

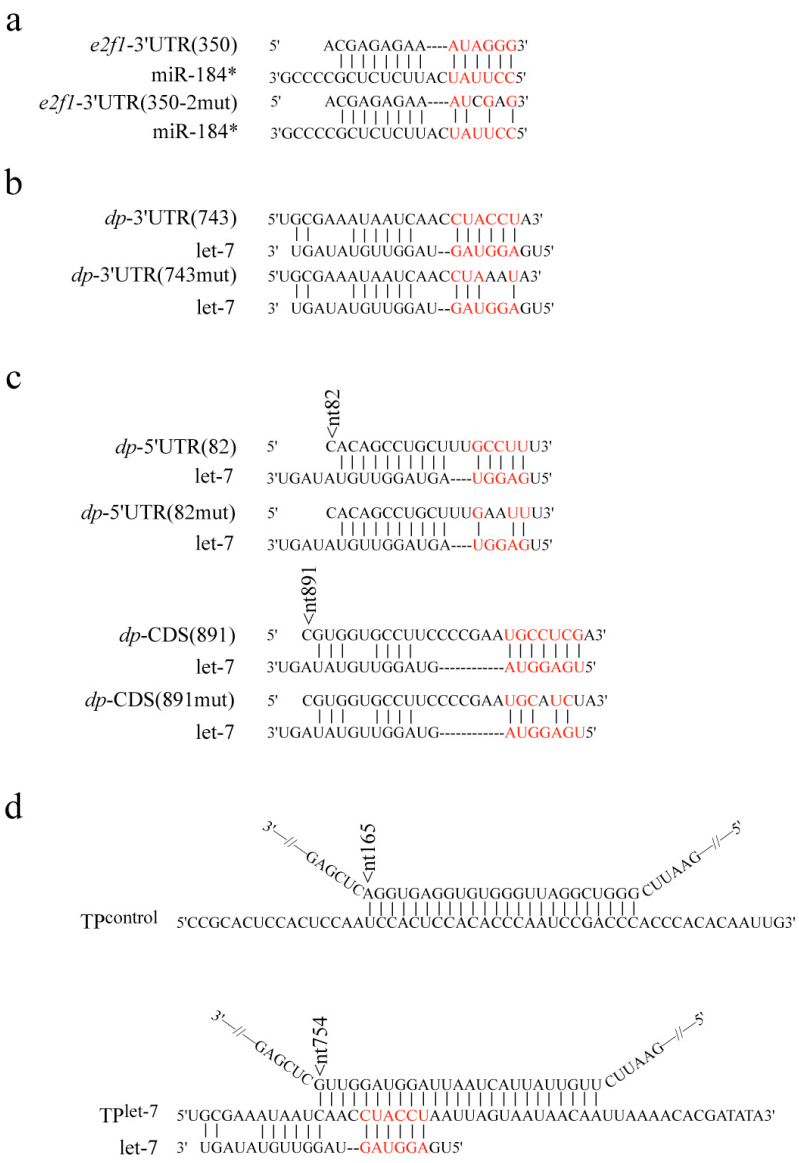

Supplementary Figure 17

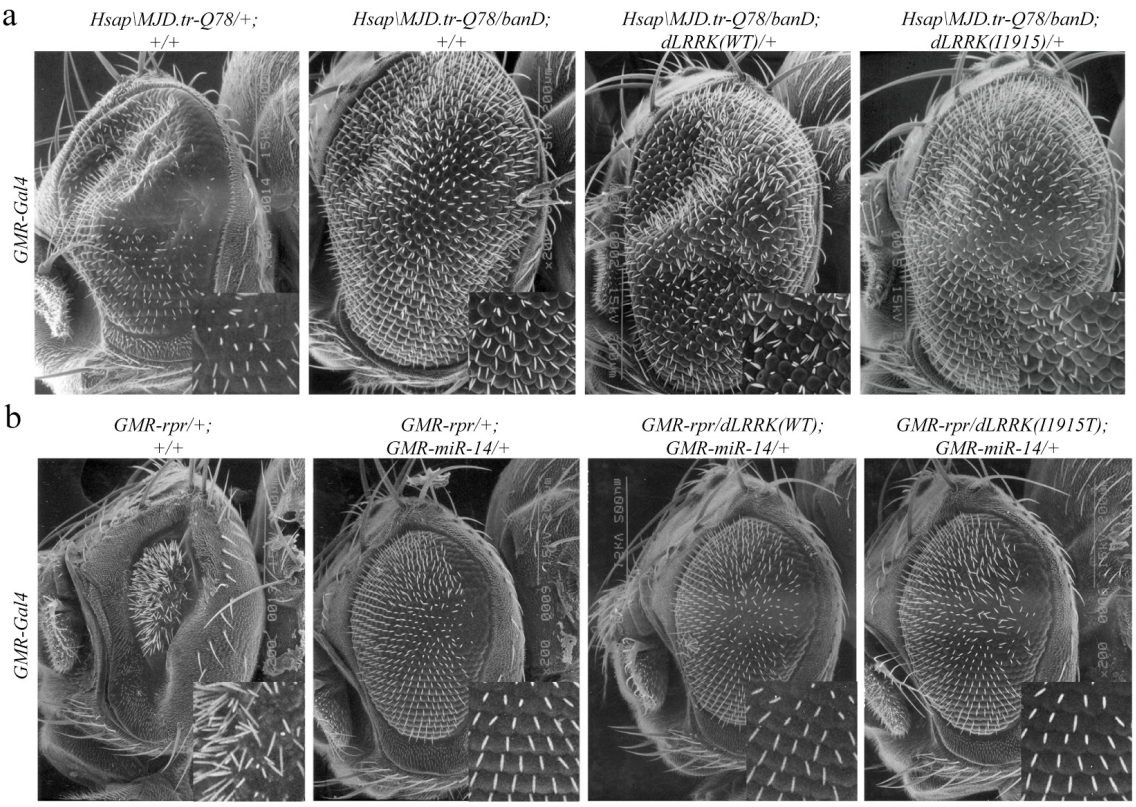

Supplementary Figure 18

a

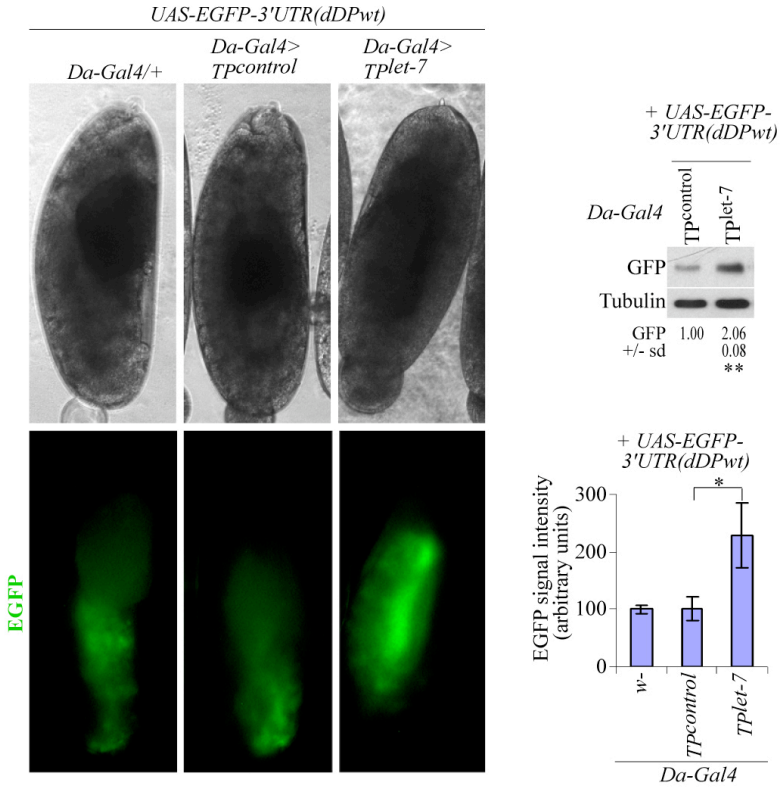

b

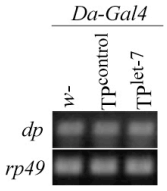

Supplementary Figure 19

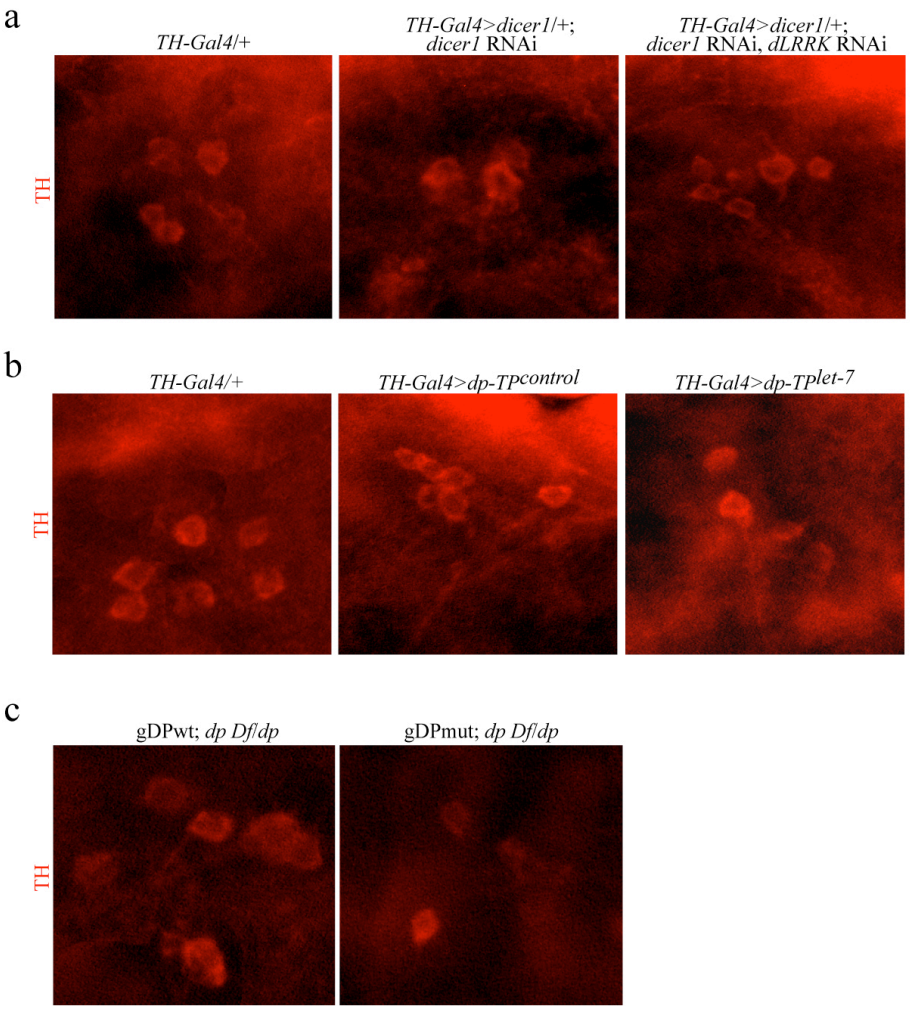

Supplementary table 1

	Da>dLRRK(I1915T) compared to *Da/+*	*Da>dLRRK(I1915T)* compared to *Da>dLRRK(WT)*
UbcD2	3.0	2.3
abdominal-A	3.2	4.0
E2f	3.9	2.5
Dp	4.2	3.1
eIF-4B	4.5	2.8
Pvr	5.5	0.5
Ribosomal L35A	5.8	6.2
Sphingosine kinase III	6.3	9.2
brat	6.6	2.1
p38a MAP kinase	7.7	4.3
Fascilin III	8.7	6.3
Wee	9.0	7.2
d-frizzle2	9.4	3.5
Ubc-E2H	9.9	5.0
Cytochrome P450A1	10.0	6.8
APC2	11.5	8.0
Atg12	12.2	9.2
LKB1	12.3	7.1
cg1139	13.9	12.2
twister	13.9	2.8